JACS
JOURNAL OF THE AMERICAN CHEMICAL SOCIETY

Article

pubs.acs.org/JACS

Structural Changes in Cytochrome *c* Oxidase Induced by Binding of Sodium and Calcium Ions: An ATR-FTIR Study

Amandine Maréchal,*[,†] Masayo Iwaki,[†,‡] and Peter R. Rich[†]

[†]Glynn Laboratory of Bioenergetics, Institute of Structural and Molecular Biology, University College London, Gower Street, London, WC1E 6BT, United Kingdom

Supporting Information

ABSTRACT: Attenuated total reflection Fourier transform infrared (ATR-FTIR) spectroscopy was used to investigate the binding of Na^+ and Ca^{2+}cations to bovine cytochrome *c* oxidase in its fully oxidized and partially reduced, cyanide-ligated ($a^{2+}a_3^{3+}$-CN) (mixed valence) forms. These ions induced distinctly different IR binding spectra, indicating that the induced structural changes are different. Despite this, their binding spectra were mutually exclusive, confirming their known competitive binding behavior. Dissociation constants for Na^+ and Ca^{2+} with the oxidized enzyme were 1.2 mM and 11 μM, respectively and Na^+ binding appeared to involve cooperative binding of two Na^+. Ca^{2+} binding induced a large IR spectrum, with prominent amide I/II polypeptide changes, bandshifts assigned to carboxylate and an arginine, and a number of bandshifts of heme *a*. The Na^+-induced binding spectrum showed much weaker amide I/II and heme *a* changes but had similar shifts assignable to carboxylate and arginine residues. Yeast C*c*O also displayed a calcium-induced IR and UV/visible binding spectra, though of lower intensities. This was attributed to the difficulty in fully depleting Ca^{2+} from its binding site, as has been found with bacterial C*c*Os. The implications of Ca^{2+}/Na^+ ion binding are discussed in terms of structure and possible modulation of core catalytic function.

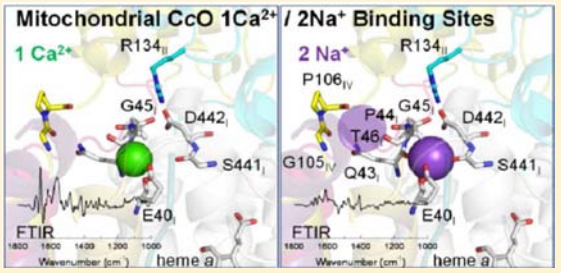

INTRODUCTION

Ca^{2+} binding to mitochondrial cytochrome *c* oxidase (C*c*O) was first detected by Wikström et al. from a Ca^{2+}-induced redshift of the Soret and α bands of reduced heme *a*.[1] Konstantinov et al. showed that this Ca^{2+}-induced redshift could be reversed by competitive binding of Na^+.[2] Titrations of both partially reduced and oxidized C*c*O suggested that the site binds either one Ca^{2+}or two Na^+ cations, with dissociation constants of 2 μM for Ca^{2+} and an average value of 3.6 mM for the two Na^+.[3,4] The binding site of one Na^+ has been identified in the atomic structure of bovine C*c*O[5] in a peptide domain of subunit I that is close to the subunit I/II interface. Coordination of Na^+ is provided by unidentate ligation from Glu40 carboxylate (2.5 Å), backbone carbonyls of Glu40 (2.3 Å), Gly45 (2.4 Å), and Ser441 (2.4 Å), and a water molecule (2.0 Å) that is H-bonded to Asp442 (3.0 Å) (Figure 1).[6]

Crystal structures of *Paracoccus denitrificans* and *Rhodobacter sphaeroides* C*c*Os revealed a Ca^{2+} ion bound in a domain equivalent to the Na^+ site of bovine C*c*O.[7,8] However, in contrast to the behavior of bovine C*c*O, no Ca^{2+}-induced redshift of reduced heme *a* was observed.[3,9] This discrepancy was resolved by metal analyses that revealed that Ca^{2+} remained bound in bacterial C*c*Os even after EDTA washing, in contrast to bovine C*c*O which retained only 0.23 Ca^{2+}/monomer.[10] Mutation of the binding site, and particularly of Asp485 in *R. sphaeroides* (Asp477 in *P. denitrificans*), weakened the binding of Ca^{2+} to an extent that it could be removed and rebound, resulting in the same Ca^{2+}-induced redshift of heme *a*.[9−11,4]

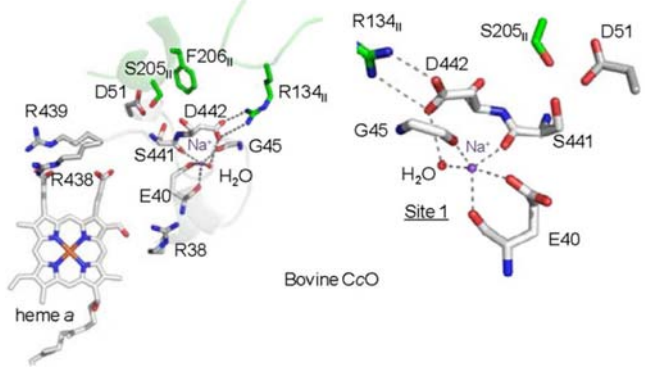

Figure 1. The crystallographically defined Na^+-binding site of bovine C*c*O. Coordination of Na^+ is provided by unidentate ligation from Glu40 carboxylate (2.5 Å), backbone carbonyls of Glu40 (2.3 Å), Gly45 (2.4 Å), and Ser441 (2.4 Å), and a water molecule (2.0 Å) that is H-bonded to Asp442 (3.0 Å) (PDB 1V54).[6]

Na^+ ions also bound to the site, though in contrast to bovine C*c*O only one Na^+ ion competed with Ca^{2+}. This suggests that these bacterial C*c*Os have a single cation binding site or that Asp485 is also required for the second Na^+ binding niche.[11,4] C*c*O of the yeast *Saccharomyces cerevisiae* also failed to show a Ca^{2+}-induced redshift of heme *a*.[3] Nevertheless, a predicted

Received: January 17, 2013
Published: March 29, 2013

   dx.doi.org/10.1021/ja4005706 | *J. Am. Chem. Soc.* 2013, 135, 5802−5807

model of its structure, based on homology modeling with the coordinates of bovine C*c*O,[12] indicates that the same Ca^{2+}/Na^{+} binding site is present. Hence, it seems likely that removal of Ca^{2+} from its binding site is also very difficult.

To date, Ca^{2+} and Na^{+} binding to C*c*Os has been measured using the electronic UV/visible changes induced in heme *a*. Attenuated total reflection-Fourier transform infrared (ATR-FTIR) difference spectroscopy has provided an alternative, widely applicable method to study ligand binding to proteins. It has been used to explore substrate binding to, for example, acetylcholine receptor,[13,14] transhydrogenase[15] and melibiose permease,[16] formate binding to C*c*O,[17] anion binding to rhodopsin,[18] heavy metal binding to cytochrome *c*[19] and cation binding to ATPase,[20] and the KcsA potassium channel.[21] In this study, perfusion-induced ATR-FTIR was used to further characterize the interactions of Na^{+} and Ca^{2+} with oxidized and partially reduced forms of bovine and yeast C*c*Os.

EXPERIMENTAL SECTION

All chemicals were purchased at their highest purity grade from Sigma-Aldrich.

Enzyme Purification and ATR-Ready Sample Preparation. Bovine heart C*c*O and six-histidine tagged yeast C*c*O were purified according to published protocols.[22,23] Their conversion to detergent-free, 'ATR-ready' forms was described previously.[24] In brief, 450 pmol of C*c*O was diluted in 20 mM KPi buffer at pH 8.0 containing 0.1% w/v sodium cholate and 0.1% w/v octyl glucoside and pelleted by centrifugation. The pellet was washed with 20 mM KPi pH 8.0 and then with 1 mM KPi buffer pH 8.0. The final material was dispersed in 5 μL of distilled water and placed on a silicon ATR prism (DuraSamp*IIR* II, SensIR/Smith Detection). After being dried with a gentle stream of N_2 gas, the protein film was rehydrated with a buffer of 100 mM KPi or MES at pH 6.5.

Cation-Induced ATR-FTIR Difference Spectroscopy. The rehydrated film was covered by a chamber that allowed buffers to be perfused over the film surface and UV/visible absorption spectra to be recorded simultaneously with IR changes.[25] ATR-FTIR spectra were recorded with a Bruker ISF 66/S spectrometer, fitted with a liquid nitrogen-cooled MCT-A detector. All frequencies quoted have accuracy to ± 1 cm^{-1}. Degassed 100 mM KPi (for Na^{+} experiments) or 100 mM MES (for Ca^{2+} experiments) at pH 6.5 was used as buffer throughout at a flow rate of 1.5 mL/min. To ensure that the C*c*O was homogeneously in the active, cation-free, "fast" oxidized form,[26] the enzyme film was first reduced and reoxidized by perfusion with 3 mM dithionite followed by 1 mM potassium ferricyanide and then washed with a buffer containing 100 μM EGTA to remove any residual cations. This was followed by buffer alone to remove residual redox chemicals and EGTA. Na^{+} and Ca^{2+} were added as NaCl and $CaCl_2$. Although the oxidized enzyme can bind chloride at the heme a_3–Cu_B site, this occurs only slowly even at high chloride concentrations[22] and is negligible at the concentrations associated with the Ca^{2+} and Na^{+} additions used here. The use of Na_2SO_4 instead of NaCl, or of MES buffer instead of KPi, produced similar Na^{+}-induced IR changes (not shown).

For measurements with the partially reduced form of the enzyme, the cation-free "fast" oxidized C*c*O was first converted to the heme a_3-cyanide ligated form by perfusion of buffer containing 500 μM KCN. This was followed by perfusion of buffer with 500 μM KCN, 200 μM ascorbic acid, and 50 μM hexaamine ruthenium(II). UV/visible and IR spectra (not shown) confirmed quantitative generation of mixed valence, cyanide-ligated ($a^{2+}a_3^{3+}$-CN) C*c*O. Cation-binding/unbinding was induced with the same buffer with/without cation(s).

For analyses of H/D exchange effects, equivalent D_2O media were used to prepare the "ATR-ready" materials and the perfusion buffers. pD values were adjusted with a standard glass pH electrode assuming pD = pH(meter reading) + 0.4.[27]

Typically, to record "cation-binding minus cation-free" difference spectra, a background spectrum (average of 500 interferograms) was recorded during perfusion of buffer containing 100 μM EGTA. The buffer was then switched to a cation-containing one and, after a 60 s delay, an equivalent sample spectrum was recorded. This process was reversed for the recording of "cation-free minus cation-binding" difference spectra. The final spectra shown are averages from 25 binding/unbinding cycles.

RESULTS AND DISCUSSION

Ca^{2+} and Na^{+} Binding to Bovine Oxidized C*c*O. Figure 2 shows the IR difference spectra induced by perfusion of Ca^{2+}- or Na^{+}-containing buffer at pH/pD 6.5 over Ca^{2+}-depleted "fast" oxidized C*c*O. Binding of 100 μM Ca^{2+} induced the characteristic UV/visible redshift of heme *a* (Figure S1, Supporting Information, top trace) whereas binding of 5 mM Na^{+} induced a small blueshift (Figure S1, lower trace) which might be due to removal of residual Ca^{2+}, even though the layer was previously washed with 100 μM EGTA.[11,4] The associated IR spectra were recorded both in H_2O and D_2O media (black and red traces in Figure 2, respectively). The IR changes induced by Ca^{2+} (trace A) are larger than, and distinctly different from, those induced by Na^{+} (trace C).

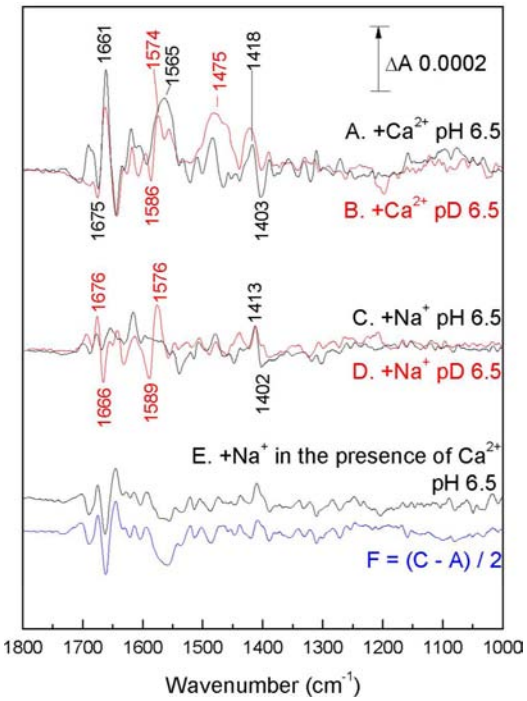

Figure 2. Ca^{2+}/Na^{+}-induced ATR-FTIR difference spectra in "fast" oxidized bovine C*c*O. Ca^{2+}-bound minus Ca^{2+}-free difference spectra were induced by perfusion of 100 μM Ca^{2+} (added as $CaCl_2$) in 100 mM MES, pH 6.5 (A) and pD 6.5 (B in red). Na^{+}-bound minus Na^{+}-free difference ATR-FTIR spectra were induced by perfusion of 4 mM Na^{+} (added as NaCl) in 100 mM KPi, pH 6.5 (C) and pD 6.5 (D in red). Na^{+}-bound minus Ca^{2+}-bound difference spectra were induced by perfusion of 5 mM Na^{+} in the presence of 25 μM Ca^{2+} in 100 mM MES, pH 6.5 (E). Trace F (blue) shows the difference of traces C and A, scaled down by a factor of 2.

Ca^{2+}-induced polypeptide backbone alterations are evident from the intense 1661(+) cm^{-1} band (trace A), whose weak sensitivity to H/D exchange is consistent with an amide I change, together with amide II absorption around 1565 cm^{-1} which shifts to around 1475 cm^{-1} in D_2O (trace B). Equivalent features were not observed on binding of Na^{+} (traces C and D). Ca^{2+} binding also induced bands at 1418(+)/1403(−) cm^{-1}

dx.doi.org/10.1021/ja4005706 | J. Am. Chem. Soc. 2013, 135, 5802−5807

(trace A) and similar bands at 1413(+)/1402(−) were induced by binding of Na^+ (trace C). These relatively large H/D-insensitive bands should arise from the ν_s of carboxylate[28] and most likely from Glu40 which is directly involved in Na^+/Ca^{2+} ligation (Figure 1).

In D_2O media, binding of Ca^{2+} or Na^+ also induces an intense trough/peak at 1586(−)/1574(+) (Ca^{2+}, trace B) or 1589(−)/1576(+) (Na^+, trace D) which most likely arise from the downshift of the ν_s vibration of a protonated arginine guanidinium group.[29] This is expected to be accompanied by a bandshift of the corresponding ν_{as} mode around 1610 cm^{-1} and, in H_2O media, ν_{as} and ν_s bandshifts around 1670 and 1635 cm^{-1}.[28] However, these will be masked by the strong amide I band changes, as evident in the Ca^{2+} binding spectra and perhaps more weakly in the Na^+ binding spectrum in D_2O (for instance the peak/trough at 1676(+)/1666(−) cm^{-1}). Candidate arginines are Arg438, Arg439, and Arg38 of subunit I or Arg134 of subunit II[5] (Figure 1). Arginines Arg438, Arg439, and Arg38 are in direct H-bonding interaction with heme *a* via its D-ring propionate or its formyl group. However, perturbation of any of these should also induce a shift of the heme *a* electronic α-band, as occurs when these are mutated in bacterial C*c*Os.[30,31] The fact that the heme *a* bandshift is only observed on Ca^{2+} binding, whereas both cation-induced IR binding spectra (traces B and D) show the same arginine perturbation, argues against their involvement. Hence, a change of Arg134 in subunit II is more plausible. Although it is located on a different peptide, its guanidinium group forms a salt bridge with Asp442 of subunit I, which would be weakened by binding of either cation in the crystallographically resolved site. Some additional, smaller bands seen in the Ca^{2+} binding spectrum most likely arise from heme *a*, and these are discussed further below.

Binding Affinities of Ca^{2+} and Na^+ to Bovine Oxidized C*c*O. Binding affinities could be estimated from plots of amplitudes of prominent IR marker bands as a function of cation concentrations (Figure 3). In the case of Ca^{2+}-binding, the 1661(+)/1675(−) cm^{-1} bandshift was used (Figure 3A). Its amplitude was almost saturated at 50−100 μM Ca^{2+} and was best fitted to a curve with a dissociation constant of 11 μM for a single binding site (red curve overlay in Figure 3A). In the case of Na^+ binding, the 1413(+)/1402(−) cm^{-1} bandshift was selected (Figure 3B). Its amplitude was almost saturated at 10−20 mM Na^+. At Na^+ concentrations above 10 mM, additional broad baseline changes were evident (not shown), which most likely arose from further structural changes due to nonspecific electrostatic effects. The data (Figure 3B) were most reasonably fitted with a dissociation constant of 1.2 mM (green curve overlay), assuming that two sodium ions bind cooperatively, as has been established from UV/visible binding data.[3] Comparison of the Na^+-induced binding spectra at different Na^+ concentrations showed that all features titrated together, indicating that the binding of the two Na^+ ions must indeed occur simultaneously in an $n = 2$ manner (if one excludes the unlikely possibility that there are two independent sites with identical binding constants). The estimated dissociation constants for Ca^{2+} and Na^+ binding to oxidized C*c*O are roughly in agreement with those of 2 μM and 3.6 mM, respectively, obtained by titrations of UV/visible redshifts.[3,4]

Competitive Binding of Ca^{2+} and Na^+ to Bovine Oxidized C*c*O. Konstantinov et al. have shown from UV/visible data that Ca^{2+} and Na^+ ion binding is competitive,[4,11] resulting in increases in their effective dissociation constants

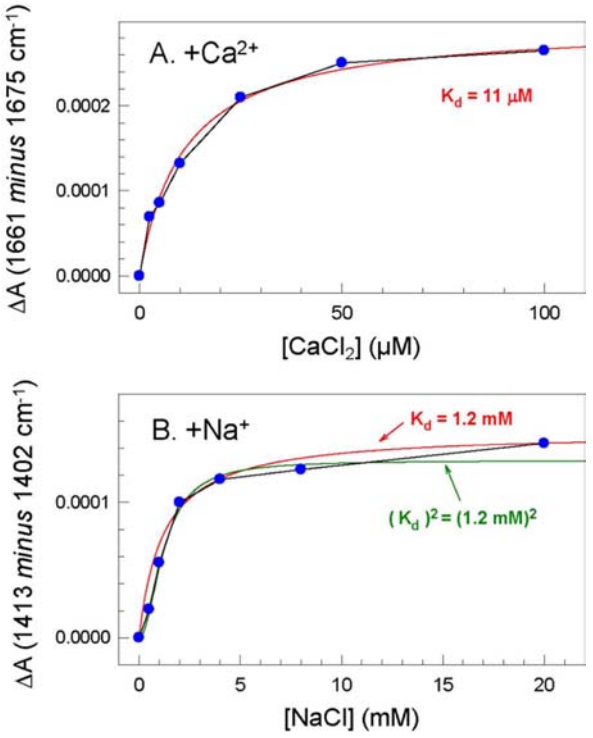

Figure 3. Titrations of IR amplitude of marker bands of Ca^{2+}/Na^+ binding to the oxidized form of bovine C*c*O. (A). IR amplitudes of the peak/trough at 1661(+)/1674(−) cm^{-1} in the Ca^{2+}-induced ATR-FTIR spectra (see Figure 2A) were plotted against the concentration of $CaCl_2$ in the perfusion buffer (100 mM MES, pH 6.5). (B). IR amplitudes of the peak/trough at 1413(+)/1402(−) cm^{-1} in the Na^+-induced ATR-FTIR spectra (see Figure 2C) were plotted against the concentration of NaCl in the perfusion buffer (100 mM KPi, pH 6.5). The fitted curves in red were calculated based on dissociation constants of 11 μM (A) and 1.2 mM (B) and assuming one cation bound per site. The curve in green (B) was calculated based on a dissociation constant of 1.2 mM and assuming concerted binding of two Na^+ cations per site.

when the other cation is present.[2,3] Although binding of a Ca^{2+} or Na^+ ion into the same site in the same C*c*O has not yet been observed by crystallography, superposition of the bovine Na^+-ligated and bacterial Ca^{2+}-ligated domains shows convincingly that the ions occupy similar, though not identical, positions that should mutually exclude each other. To confirm this, the difference spectrum induced by binding of Na^+ to C*c*O with bound Ca^{2+} was recorded by perfusion of 5 mM NaCl over "fast" oxidized C*c*O in the presence of 25 μM Ca^{2+} (trace E, Figure 2). This spectrum closely resembles the Na^+ binding spectrum (trace C) superimposed on the inverse of the Ca^{2+} binding spectrum (trace A), i.e., "trace C minus trace A" (trace F, scaled down by a factor of 2 to match the signal intensity in trace E). Hence, the binding of Na^+- to Ca^{2+}-saturated C*c*O results in displacement of bound Ca^{2+}. This confirmed that Na^+ and Ca^{2+} bind competitively to oxidized C*c*O, consistent with their binding to overlapping, mutually exclusive sites.

Ca^{2+} and Na^+ Binding to Partially Reduced, Cyanide-Ligated Bovine C*c*O. To assess whether any vibrational changes arose from heme *a*, the influence of heme *a* redox state on binding spectra was assessed. The partially reduced, cyanide-ligated ($a^{2+}a_3^{3+}$-CN) form (Figure S2, Supporting Information) was generated by perfusion of oxidized C*c*O with potassium cyanide and ascorbic acid/hexaamine ruthenium(II). Addition

dx.doi.org/10.1021/ja4005706 | J. Am. Chem. Soc. 2013, 135, 5802−5807

of 100 μM Ca^{2+} induced the expected redshifts of the heme *a* Soret- and α-bands[1,3] (Figure S3, Supporting Information). The associated IR spectrum (trace B of Figure 4) is similar to

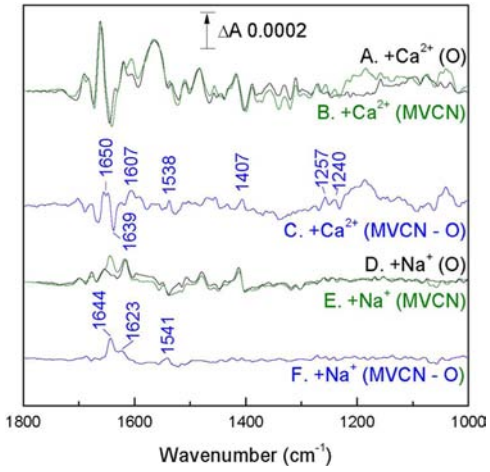

Figure 4. Ca^{2+}/Na^{+}-induced ATR-FTIR difference spectra in the mixed valence, cyanide ligated form of bovine C*c*O: comparison with cation binding to oxidized C*c*O. To generate and maintain the mixed valence state (in which heme a_3 is cyanide-ligated and oxidized and heme *a* is reduced) buffers additionally contained 500 μM potassium cyanide, 200 μM ascorbic acid, and 50 μM hexaamine ruthenium(II) chloride. Ca^{2+}-bound minus Ca^{2+}-free difference spectra were induced by perfusion of 100 μM $CaCl_2$ in 100 mM MES pH 6.5 over the oxidized (A in black, reproduced from Figure 2) or the mixed valence, cyanide ligated (B in green) forms of bovine C*c*O. Trace C shows the double difference spectrum of B minus A (in blue). Na^{+}-bound minus Na^{+}-free difference ATR-FTIR spectra were induced by perfusion of 5 mM NaCl in 100 mM KPi pH 6.5 over the oxidized (D in black, reproduced from Figure 2) or the mixed valence, cyanide-ligated (E in green) forms of bovine C*c*O. Trace F shows the double difference spectrum of E minus D (in blue).

that obtained with oxidized C*c*O (trace A of Figure 4) but with several relatively small, consistent differences. A number of these are at frequencies expected for heme substituent/macrocycle vibrations. For example, a positive band at 1607 cm^{-1} in the ($a^{2+}a_3^{3+}$-CN) form, possibly replacing one at around 1639 cm^{-1} in oxidized C*c*O (trace C of Figure 4), most likely arises from perturbation of the heme *a* formyl group, which shifts from 1650 to 1610 cm^{-1} when heme *a* changes from its oxidized to reduced state.[32,11] Positives at 1538, 1407, 1257, and 1240 cm^{-1} are frequencies at which H/D-insensitive heme macrocycle vibrations are known to occur. Overall, these heme *a* redox state-dependent changes provide direct support, consistent with the redshifts of the electronic bands, that binding of Ca^{2+} influences the electronic structure of heme *a*.

The spectrum induced by binding of Na^{+} to partially reduced cyanide-ligated C*c*O (trace E of Figure 4) was much more similar to that obtained with oxidized C*c*O (as seen from the comparison of the difference spectra presented as traces C and F of Figure 4). Weak differences in the amide I and II regions are evident together with some very weak heme macrocycle band changes, consistent with the fact that Na^{+} does not induce electronic bandshifts of heme *a*.

Competition of Ca^{2+} and Na^{+} for the same binding site could again be demonstrated by perfusion of 5 mM Na^{+} in the presence of 25 μM Ca^{2+}. The associated IR spectrum (trace E in Figure S2 with corresponding visible data in Figure S3), corresponds to the Na^{+} binding spectrum superimposed on the inverse of the Ca^{2+} binding spectrum (Figure S2, trace F representing 'trace C minus trace A', scaled to match the signal intensity of the recorded trace E).

Ca^{2+} and Na^{+} Binding to Yeast C*c*O. Ca^{2+} and Na^{+} binding spectra were also generated with yeast C*c*O. Figure 5

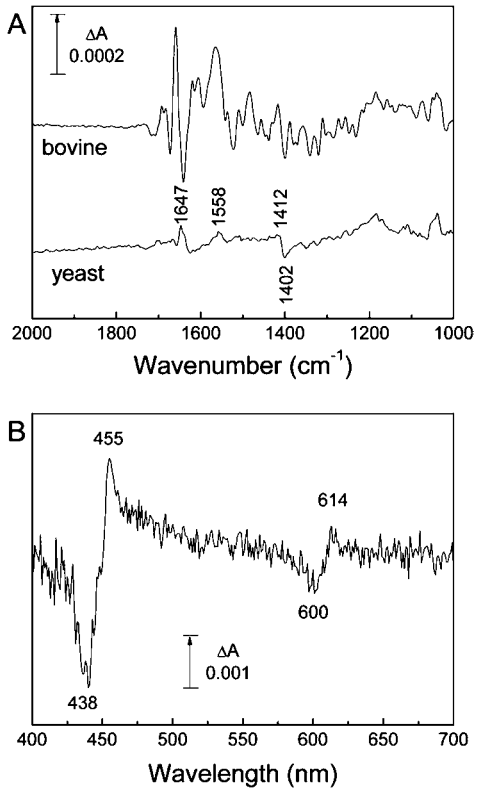

Figure 5. Ca^{2+} binding to yeast C*c*O. (A) Ca^{2+}-induced ATR-FTIR difference spectra in the mixed valence forms of bovine (top trace, reproduced from Figure 4) and yeast WT (lower trace) C*c*Os. Ca^{2+}-bound minus Ca^{2+}-free difference spectra were induced by perfusion of 100 (bovine) and 200 (yeast) μM $CaCl_2$ in 100 mM MES pH 6.5 containing 500 μM potassium cyanide, 200 μM ascorbic acid, and 50 μM hexaamine ruthenium(II) chloride. (B). UV/visible difference spectrum measured simultaneously with the IR changes induced by binding of Ca^{2+} to mixed valence yeast WT C*c*O.

presents the spectral changes induced by perfusion of 200 μM Ca^{2+} over partially reduced CN-ligated yeast oxidase at pH 6.5 after washing with 500 μM EGTA. Figure 5B shows the expected redshift of heme *a* Soret and α bands, though with intensities of only 20% of those of the equivalent binding spectrum of bovine C*c*O (Figure S3). The associated IR spectrum (Figure 5A) is also approximately 20% of the intensity of that of bovine C*c*O and is dominated by amide I/II changes at 1647(+) and 1558(+) cm^{-1} and a carboxylate change at 1402(−) and possibly 1412(+) cm^{-1}. A similar IR difference spectrum was induced with Ca^{2+} binding to oxidized yeast C*c*O (not shown). No IR or visible changes could be detected with confidence on perfusion of Na^{+}-containing buffer. These results suggest that the same cation binding site in yeast C*c*O is indeed present[12] but, like bacterial C*c*Os, it is much more difficult to deplete it of endogenously bound Ca^{2+} ions.

Conclusions and Mechanistic Relevance. The model that emerges is a binding site which, when binding Ca^{2+}, induces polypeptide backbone changes, perturbation of

dx.doi.org/10.1021/ja4005706 | J. Am. Chem. Soc. 2013, 135, 5802−5807

carboxylate (probably Glu40) and an arginine (probably Arg134 of subunit II), and longer range effect on heme *a*, most notably seen in perturbation of the heme *a* formyl band and changes in the heme macrocycle ring modes. The bound cation is not in direct contact with heme *a*. Its effects may be transmitted through nearby Tyr54, which is in H-bonding contact with the A-ring propionate of heme *a*. Alternatively, long-range effects may be transmitted to heme *a* through modulation of the dielectric properties of part of the hydrophilic H-channel.[33] For example, H-channel residues Asn451, Arg38, Tyr371, and Gln428 and associated water molecules directly link the cation site to heme *a* and its formyl group.[6] A charge change at the cation site could induce dielectric changes in these residues, which in turn would influence the net charge around, and the spectroscopic properties of, heme *a*.

A sodium ion competes for this same site but has rather weak effects on polypeptide and heme *a*, perhaps because only a single positive charge is introduced into the common Ca^{2+}/Na^{+} binding location. It is linked in bovine C*c*O with co-operative binding of a second Na^{+} whose location has not been identified. It has been suggested that Asp442, Asp51, Ser441, Ser205, and Phe206 of subunit II could form the second Na^{+} binding site.[4] In oxidized C*c*O, Asp51 is protonated with its COOH absorbing at 1737 cm^{-1} but becomes deprotonated when heme *a* is reduced and the 1737 cm^{-1} band is lost.[34] Hence, if it were to contribute to the second Na^{+} binding site, some shift of the 1737 cm^{-1} band might be expected in the binding spectrum to oxidized C*c*O, which should be lost and replaced by shifts of carboxylate bands in the partially reduced form. However, such bands are not evident (Figure 2, trace C). In addition, if Asp51 were involved in cation binding, a sodium- or calcium-induced alteration of its 1737 cm^{-1} band that appears in redox difference spectra[34,35] might be expected. This was addressed in the experiment shown in Figure 6; again, it is clear that binding of these cations does not influence this residue. Hence, the IR data do not support a direct role for Asp51 in the second Na^{+} binding site. In mitochondrial forms of C*c*O, the first Na^{+} binding site closely interacts with a domain of supernumerary subunit IV. It is possible that the second Na^{+} binding site in bovine mitochondrial C*c*O could instead be located at this subunit I/IV interface. For instance, it could be formed with the backbone carbonyl of Thr46, Pro44, and the side chain of Gln43 of subunit I and the backbone carbonyl of Pro106 or Gly105 of subunit IV (Figure S4, Supporting Information). The absence of supernumerary subunits in bacterial C*c*Os would explain why this second cooperative Na^{+} site is absent.

The physiological significance of the Ca^{2+}/Na^{+} binding sites remains unclear, particularly because the cation sites do not directly interact with the metal cofactors.[5] In the case of bovine C*c*O, it was speculated that the Na^{+} site might be involved in proton pumping by forming part of the proton exit route of the H pathway.[3,36] It was also proposed that a sodium ion in the common Ca^{2+}/Na^{+} site was energetically essential for this proton transfer step.[37] Other intriguing suggestions are that the site might provide a gated pathway for proton uncoupling at high proton motive force and/or a site for cation-influenced protein phosphorylation control.[4] Several groups were unable to find any effect on proton translocation or catalytic turnover number[9,10] though, more recently, tissue-dependent inhibitory effects of Ca^{2+} on rat C*c*O when turning over slowly have been reported.[38] This latter group have also reported that Ca^{2+} binding alters the heme *a* redox potential and slows internal electron transfer to heme a_3.[39] Hence, ion binding to this site, perhaps with the involvement of tissue-dependent supernumerary subunit IV as suggested here, might act as a fine-tuning regulator of core aspects of enzyme function through alteration of properties around heme *a*, mediated through modulation of the dielectric properties of the H-channel.[33] This aspect is currently under investigation.

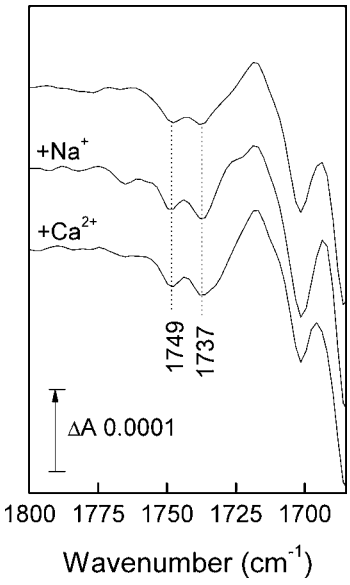

Figure 6. Effects of bound Ca^{2+} or Na^{+} on the redox-linked carboxylic acid groups of bovine C*c*O. Reduced minus oxidized ATR-FTIR difference spectra were recorded in 100 mM MES at pH 6.5 on EGTA-washed, cation-depleted C*c*O (upper trace) and in the presence of 4 mM NaCl (middle trace) or $CaCl_2$ (lower trace). The fully oxidized and fully reduced states of C*c*O were formed by perfusion with buffer containing 1 mM ferricyanide or 3 mM dithionite, respectively. Redox cycles were repeated four times, and reductive and oxidative spectra were averaged to produce the final spectra, which are plotted in the 1800−1700 cm^{-1} range where protonated carboxyl groups absorb.

■ ASSOCIATED CONTENT

Supporting Information

UV/visible difference spectra recorded simultaneously to all IR data. Cation-induced ATR-FTIR difference spectra in the cyanide-ligated and partially reduced form of bovine C*c*O. Representation of the proposed second Na^{+} binding site of bovine C*c*O, at the interface of subunits I and IV. This material is available free of charge via the Internet at http://pubs.acs.org.

■ AUTHOR INFORMATION

Corresponding Author

a.marechal@ucl.ac.uk

Present Address

‡Department of Frontier Materials, Nagoya Institute of Technology, Showa-ku, Nagoya 466-8555, Japan.

Notes

The authors declare no competing financial interest.

■ ACKNOWLEDGMENTS

We are grateful to Dr. Brigitte Meunier for providing the histidine-tagged yeast enzyme strain and to Mr. Santiago Garcia for specialist electronic and mechanical support. This work is

funded by the Biotechnology and Biological Sciences Research Council (grant code BB/K001094/1).

REFERENCES

(1) Wikström, M.; Saari, H. *Biochim. Biophys. Acta* **1975**, *408*, 170.
(2) Mkrtchyan, H.; Vygodina, T.; Konstantinov, A. *Biochem. Int.* **1990**, *20*, 183.
(3) Kirichenko, A.; Vygodina, T.; Mkrtchyan, M.; Konstantinov, A. *FEBS Lett.* **1998**, *423*, 329.
(4) Kirichenko, A. V.; Pfitzner, U.; Ludwig, B.; Soares, C. M.; Vygodina, T. V.; Konstantinov, A. A. *Biochemistry* **2005**, *44*, 12391.
(5) Yoshikawa, S.; Shinzawa-Itoh, K.; Nakashima, R.; Yaono, R.; Yamashita, E.; Inoue, N.; Yao, M.; Fei, M. J.; Libeu, C. P.; Mizushima, T.; Yamaguchi, H.; Tomizaki, T.; Tsukihara, T. *Science* **1998**, *280*, 1723.
(6) Tsukihara, T.; Shimokata, K.; Katayama, Y.; Shimada, H.; Muramoto, K.; Aoyama, H.; Mochizuki, M.; Shinozawa-Itoh, K.; Yamashita, E.; Yao, M.; Ishimura, Y.; Yoshikawa, S. *Proc. Natl. Acad. Sci. U.S.A.* **2003**, *100*, 15304.
(7) Svensson-Ek, M.; Abramson, J.; Larsson, G.; Törnroth, S.; Brzezinski, P.; Iwata, S. *J. Mol. Biol.* **2002**, *321*, 329.
(8) Ostermeier, C.; Harrenga, A.; Ermler, U.; Michel, H. *Proc. Natl. Acad. Sci. U.S.A.* **1997**, *94*, 10547.
(9) Riistama, S.; Laakkonen, L.; Wikström, M.; Verkhovsky, M. I.; Puustinen, A. *Biochemistry* **1999**, *38*, 10670.
(10) Pfitzner, U.; Kirichenko, A.; Konstantinov, A. A.; Mertens, M.; Wittershagen, A.; Kolbesen, B. O.; Steffens, G. C. M.; Harrenga, A.; Michel, H.; Ludwig, B. *FEBS Lett.* **1999**, *456*, 365.
(11) Lee, A.; Kirichenko, A.; Vygodina, T.; Siletsky, S. A.; Das, T. K.; Rousseau, D. L.; Gennis, R.; Konstantinov, A. A. *Biochemistry* **2002**, *41*, 8886.
(12) Maréchal, A.; Meunier, B.; Lee, D.; Orengo, C.; Rich, P. R. *Biochim. Biophys. Acta, Bioenerg.* **2012**, *1817*, 620.
(13) Baenziger, J. E.; Miller, K. W.; Rothschild, K. J. *Biophys. J.* **1992**, *61*, 983.
(14) Baenziger, J. E.; Miller, K. W.; Rothschild, K. J. *Biochemistry* **1993**, *32*, 5448.
(15) Iwaki, M.; Cotton, N. P. J.; Quirk, P. G.; Rich, P. R.; Jackson, J. B. *J. Am. Chem. Soc.* **2006**, *128*, 2621.
(16) León, X.; Lemonnier, R.; Leblanc, G.; Padrós, E. *Biophys. J.* **2006**, *91*, 4440.
(17) Iwaki, M.; Rich, P. R. *J. Am. Chem. Soc.* **2004**, *126*, 2386.
(18) Guijarro, J.; Engelhard, M.; Siebert, F. *Biochemistry* **2006**, *45*, 11578.
(19) Gourion-Arsiquaud, S.; Chevance, S.; Bouyer, P.; Garnier, L.; Montillet, J.-L.; Bondon, A.; Berthomieu, C. *Biochemistry* **2005**, *44*, 8652.
(20) Furutani, Y.; Murata, T.; Kandori, H. *J. Am. Chem. Soc.* **2011**, *133*, 2860.
(21) Furutani, Y.; Shimizu, H.; Asai, Y.; Fukuda, T.; Oiki, S.; Kandori, H. *J. Phys. Chem. Lett.* **2012**, *3*, 3806.
(22) Moody, A. J.; Cooper, C. E.; Rich, P. R. *Biochim. Biophys. Acta* **1991**, *1059*, 189.
(23) Meunier, B.; Maréchal, A.; Rich, P. R. *Biochem. J.* **2012**, *444*, 199.
(24) Iwaki, M.; Puustinen, A.; Wikström, M.; Rich, P. R. *Biochemistry* **2003**, *42*, 8809.
(25) Rich, P. R.; Iwaki, M. *Mol. Biosyst.* **2007**, *3*, 398.
(26) Moody, A. J. *Biochim. Biophys. Acta* **1996**, *1276*, 6.
(27) Glasoe, P. K.; Long, F. A. *J. Phys. Chem.* **1960**, *64*, 188.
(28) Barth, A. *Prog. Biophys. Mol. Biol.* **2000**, *74*, 141.
(29) Iwaki, M.; Rich, P. R. *J. Am. Chem. Soc.* **2007**, *129*, 2923.
(30) Riistama, S.; Verkhovsky, M.; Laakkonen, L.; Wikström, M.; Puustinen, A. *Biochim. Biophys. Acta, Bioenerg.* **2000**, *1456*, 1.
(31) Lee, H. J.; Ojemyr, L.; Vakkasoglu, A.; Brzezinski, P.; Gennis, R. B. *Biochemistry* **2009**, *48*, 7123.
(32) Callahan, P. M.; Babcock, G. T. *Biochemistry* **1983**, *22*, 452.
(33) Rich, P. R.; Maréchal, A.; Meunier, B.; Dodia, R. *Biochim. Biophys. Acta, Bioenerg.* **2012**, *1817*, S102.
(34) Okuno, D.; Iwase, T.; Shinzawa-Itoh, K.; Yoshikawa, S.; Kitagawa, T. *J. Am. Chem. Soc.* **2003**, *125*, 7209.
(35) Rich, P. R.; Maréchal, A. *Biochim. Biophys. Acta, Bioenerg.* **2008**, *1777*, 912.
(36) Yoshikawa, S.; Muramoto, K.; Shinozawa-Itoh, K.; Aoyama, H.; Tsukihara, T.; Shimokata, K.; Katayama, Y.; Shimada, H. *Biochim. Biophys. Acta* **2006**, *1757*, 1110.
(37) Kamiya, K.; Boero, M.; Tateno, M.; Shiraishi, K.; Oshiyama, A. *J. Am. Chem. Soc.* **2007**, *129*, 9663.
(38) Vygodina, T. V.; Konstantinov, A. A. *Biochim. Biophys. Acta, Bioenerg.* **2010**, *1797*, 102.
(39) Vygodina, T. V.; Dyuba, A. V.; Konstantinov, A. A. *Biochemistry (Moscow)* **2012**, *77*, 901.